

## Water in Contact with Extended Hydrophobic Surfaces: Direct Evidence of Weak Dewetting

Torben R. Jensen,<sup>1,\*</sup> Morten Østergaard Jensen,<sup>2,†</sup> Niels Reitzel,<sup>3</sup> Konstantin Balashev,<sup>3</sup> Günther H. Peters,<sup>2</sup>  
Kristian Kjaer,<sup>1</sup> and Thomas Bjørnholm<sup>3,‡</sup>

<sup>1</sup>Materials Research Department, Risø National Laboratory, DK-4000 Roskilde, Denmark

<sup>2</sup>Department of Chemistry, Technical University of Denmark, DK-2800 Lyngby, Denmark

<sup>3</sup>Nano-Science Center, Department of Chemistry, University of Copenhagen, Universitetsparken 5, DK-2100 Ø, Denmark

(Received 24 April 2002; published 27 February 2003)

X-ray reflectivity measurements reveal a significant dewetting of a large hydrophobic paraffin surface floating on water. The dewetting phenomenon extends less than 15 Å into the bulk water phase and results in an integrated density deficit of about one water molecule per 25–30 Å<sup>2</sup> of water in contact with the paraffin surface. The results are supported by molecular dynamics simulations and related to the hydrophobic effect.

DOI: 10.1103/PhysRevLett.90.086101

PACS numbers: 68.08.Bc, 61.10.Kw, 61.30.Hn

The nature of the contact region between water and a hydrophobic surface has long been recognized to hold the key to the understanding of the hydrophobic effect [1–11] which plays an important role for phenomena as diverse as protein folding, lipid aggregation, forces between hydrophobic surfaces in water, or chemical self-assembly of macroscopic objects [12]. For highly curved molecular surfaces water molecules are believed to form ordered hydrogen bonded structures around the solute [11,13] while more extended surfaces seriously disrupt the hydrogen bonding patterns [14,15]. In the latter case, pertaining to surfaces with radii of curvature greater than 1 nm [3,16], a number of theoretical papers have suggested that dewetting plays an important role [1–7] and a number of experiments involving two hydrophobic surfaces in close contact have shown that significant dewetting of the contact region takes place (cavitation) as also expected for a narrow hydrophobic capillary [17].

We provide here the first quantitative experimental evidence of dewetting of a single hydrophobic surface in contact with water. The magnitude of the effect is significantly smaller than suggested by Stillinger in 1973 [1] and more recently by Lum, Chandler, and Weeks [3], showing that a complete dewetting, resulting in a water vapor interfacial region extending over many molecular layers, does not take place at hydrophobic surfaces. We estimate that the presence of the density deficit may nevertheless explain the major component to the hydrophobic interfacial energy as simply due to the isothermal decompressibility of water at the interface.

Our results are based on measurements of the x-ray reflectivity (XR) of a pure water surface covered with a 2D-crystalline monolayer of the *n*-alkane *n*-C<sub>36</sub>H<sub>74</sub> [18], as a function of the angle of incidence [19]. The experiment was performed at the beam line BW1 at DESY in Hamburg and experimental details follow Ref. [18] closely. Because of interference between x rays reflected from different depths in the interfacial region [19], the reflectivity, normalized to the Fresnel reflectivity of bare water, is found to oscillate strongly as a function of the

angle of incidence [Fig. 1(a)]. By a model independent inversion of the data [21] it is possible to determine the normalized electron density profile,  $\rho(z)/\rho_{\text{water}}$ , across the interface. The result is shown in Fig. 1(b), where a shaded area indicates a decrease in the density down to about  $\rho(z)/\rho_{\text{water}} = 0.9$  occurring at the hydrophobic interface. The contact region with low water density, which is smeared by the roughness of the water surface (cf. below), has a half width of 8–10 Å.

The electron density of bulk crystalline alkanes is similar to that of water ( $\rho_{\text{alkane}}/\rho_{\text{water}} = 1.03$ ) and the density profile inverted from the XR data [Fig. 1(b)] indeed reaches unity in that part of the  $\approx 40$  Å thick paraffin monolayer which is closest to the water surface. However, farther away from the water surface the electron density decays to a plateau at 73% of this value. A plausible interpretation is that at these distances, but not at the very interface, the monolayer contains holes with a less dense packing of the paraffin molecules, as schematically illustrated in Fig. 1(c) (zone II). The fraction of these holes is sensitive to temperature, lateral pressure, and spreading conditions, while the alkane electron density always reaches unity at the very interface. The dip in the water density at the alkane/water interface is therefore always distinct, and it is found to be relatively insensitive to the parameters mentioned above. This was to be expected because both the crystalline phase, which gives rise to distinct diffraction [18], [zone I, Fig. 1(c)] and the presumed disordered phase [zone II, Fig. 1(c)] are both hydrophobic at the water interface. Because of the (inherent) roughness of the water surface of about 3 Å [root mean square (rms)] caused by thermally excited capillary waves [19], the experimental data cannot clearly distinguish between a narrow deep dip or a shallow wider dip with the same integrated density deficit  $D_{\text{exp}} = \int \Delta\rho(z)dz$ , where  $\Delta\rho(z)$  denotes the difference between (i) the densities represented by a smooth line connecting the bulk water and bulk paraffin densities and (ii) the measured density. Nevertheless, the data clearly show that the density effect has a range of less than  $\approx 15$  Å

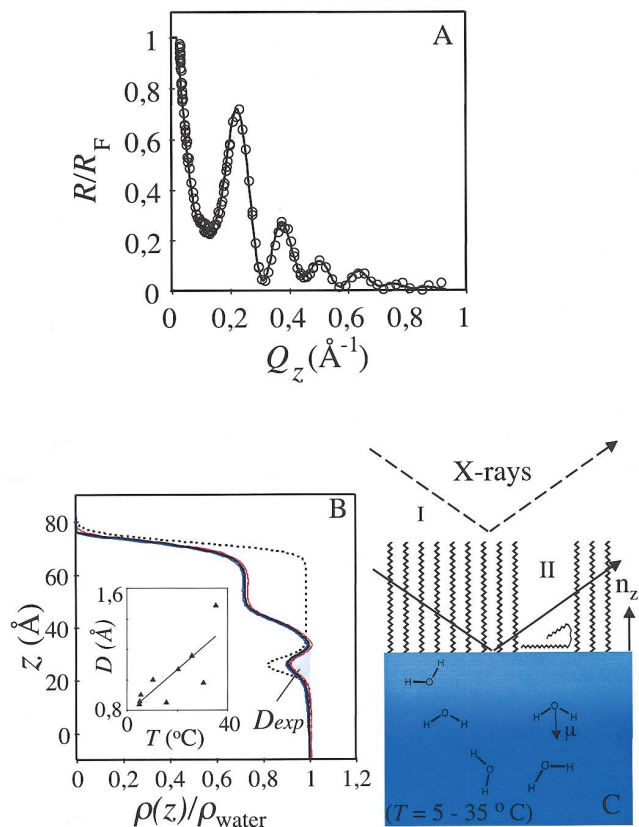


FIG. 1 (color). (a) X-ray reflectivity of a paraffin monolayer on water, normalized to the Fresnel reflectivity for bare water, versus scattering vector  $Q_z = 4\pi \sin(\alpha)/\lambda$  where  $\alpha$  is the grazing angle of incidence. (b) Experimental (solid line, zone I + II) and modeled electron density (dotted line, zone I) corresponding to the data shown in (a). Error bands (red and blue solid lines) are calculated according to [20]. The inset shows (points) the integrated electron deficit,  $D$ , as a function of temperature while the solid line is a linear fit to the data provided as a guide to the eye only. (c) Schematic illustration of the experimental results.

indicating that this is the upper limit to the range of the dewetting phenomena.

To complement our observation of the density deficit we have extended the experiments to include monolayers of a series of other less hydrophobic molecules. In Fig. 2 the resulting values of  $D_{\text{exp}}$  are plotted versus the degree of hydrophobicity expressed in terms of the water drop contact angle,  $\beta$ , as measured on self-assembled close-packed monolayers exposing the relevant moieties towards a solid-air interface [22]. Our results show a density deficit for paraffin only. At the same time, paraffin is the only substance in the series that has an advancing contact angle greater than  $90^{\circ}$ , which marks the transition from a net attractive to net repulsive interfacial interaction between the solid and the liquid as implied by Young's equation [10]  $\cos(\beta) = (\gamma_{sa} - \gamma_{sl})/\gamma_{la}$  where the  $\gamma_{xy}$  denote the interfacial tensions between the media: solid ( $s$ ), air ( $a$ ), and liquid ( $l$ ). The results thus strongly indicate that dewetting is a microscopic expression of the

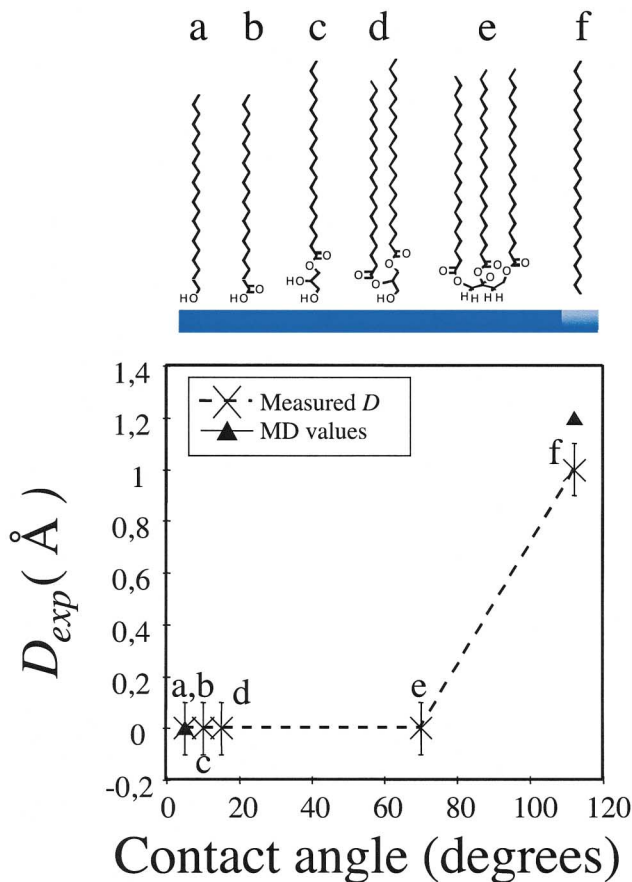


FIG. 2 (color). Integrated electron deficit,  $D$ , measured by x-ray reflectivity of a solid-water interface (Langmuir film) as a function of the estimated (advancing) water drop contact angle of the equivalent solid-air interface. *a*: 1-triacontanol ( $\text{C}_{30}\text{H}_{61}\text{OH}$ ); *b*: fatty acid; *c*: monopalmitoyl glycerol ester; *d*: dipalmitoyl glycerol ester; *e*: tripalmitoyl glycerol ester; *f*: hexatriacontane. Contact angles are taken from Ref. [22].  $D$  values represent our own data. The MD (molecular dynamics) values are for *a*: 1-pentatriacontanol ( $\text{C}_{35}\text{H}_{71}\text{OH}$ ) and *f*: hexatriacontane. The dotted line is a guide to the eye.

macroscopic transition from net attractive to net repulsive interfacial interactions.

The temperature dependence of  $D_{\text{exp}}$  for paraffin shows that  $D_{\text{exp}}$  increases by 10%–30% when temperatures increase from 5 to  $35^{\circ}\text{C}$  [Fig. 1(b) inset]. This is the trend predicted by simple solvophobic density depression models [23] which treat the water molecules as spheres interacting through a simple Lennard-Jones potential and having only repulsive interactions with the solid surface.

To gain further insight into the dewetting phenomena and the interfacial water structure, we have performed molecular dynamics (MD) simulations on a periodic alkane-water system ( $\text{C}_{36}\text{H}_{74}/\text{H}_2\text{O}/\text{C}_{36}\text{H}_{74}$ ) counting  $\sim 45\,000$  atoms, Fig. 3, using the program NAMD [24] and the full atomistic CHARMM22 force field [25]. The simulations were carried out at constant pressure (1 atm) and temperature (300 K). Electrostatic forces were computed with the Particle Mesh Ewald method [26] (details

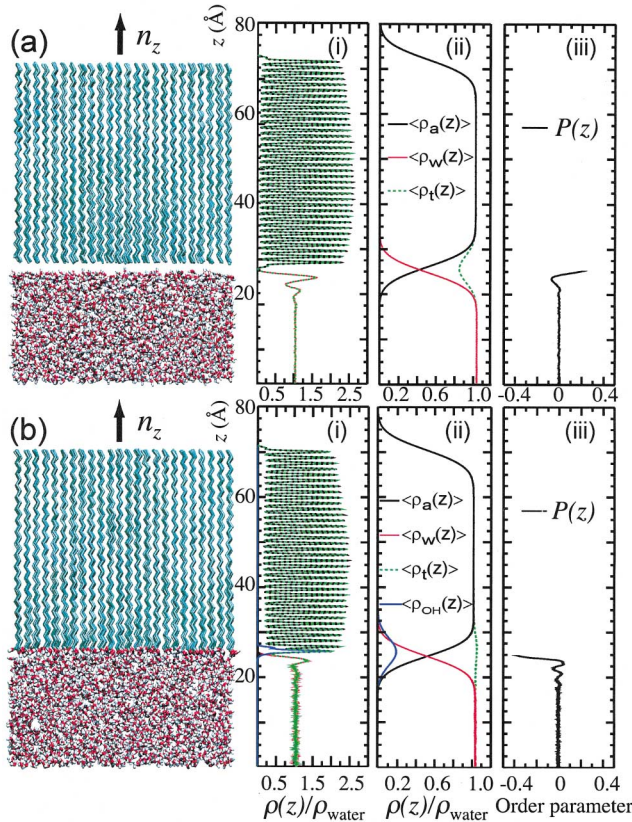


FIG. 3 (color). Snapshots of half of the symmetric alkane/water/alkane (a) and alcohol/water/alcohol (b) systems taken after 1 ns of molecular dynamics simulation conducted at constant temperature and pressure. The alkane and alcohol layers are shown without aliphatic hydrogen atoms and are colored cyan. The hydroxyl group of the alcohol layer is displayed in licorice with O and H atoms colored red and white, respectively. Water is shown in the same representation. Panels (i) show the unsmeared electron density profile ( $\langle \rho_f(z) \rangle$ ) normalized by the electron density of bulk water at 300 K, 1 atm ( $0.333 \text{ \AA}^{-3}$ ) and decomposed into contributions from alkane or alcohol ( $\langle \rho_a(z) \rangle$ ), water ( $\langle \rho_w(z) \rangle$ ) and, for the alcohol layer, from the hydroxyl group ( $\langle \rho_{OH}(z) \rangle$ ), see panels (ii) for legends. Panels (ii) show the same quantities smeared by  $3 \text{ \AA}$ . Panels (iii) depict the water ordering through the order parameters  $P(z) = \langle \cos(\theta) \rangle$  where  $\theta$  is the angle between the water dipole (unit) vector and the surface normal along  $z$ ,  $n_z$ , which is displayed above the alkane/alcohol layers.  $\theta'$  is the angle between the vector  $r_{OH}(z) = r_H(z) - r_O(z)$  and  $n_z$ . All data were averaged over the last 750 ps of the trajectories.

submitted for publication elsewhere [27]). Figure 1(b) compares the MD results (dotted line) with the density profile inverted from the XR data (full line). The calculated density has been smeared by a rms roughness of  $3 \text{ \AA}$  to allow direct comparison with the experimental curve. It can be seen that the width of the crystalline paraffin monolayer (zone I) determined from the simulations reproduces the measured width of the monolayer. Furthermore the electron density calculated from the simulations reproduces the interfacial density deficit quite accurately. This is in accordance with some previous simulation

studies [4,5]. Details of our calculated density decrease are found in Fig. 3(a) which shows a snapshot of the molecular models as well as the calculated density that is further separated into two contributions stemming from the paraffin and water phases, respectively. According to the simulations  $D$  results from a narrow and deep electron density deficit [Fig. 3(a)] indicating that the broader and shallower dip found experimentally is due to the smearing of the interface caused by capillary waves. The calculated value of  $D_{MD} = 1.2 \text{ \AA}$  is about 20% larger than the measured value,  $D_{exp} = 1 \text{ \AA}$  (Fig. 2). As a second reference point also included in the comparisons in Fig. 2, MD simulations of a periodic 1-pentatriacontanol-water system ( $C_{35}H_{71}OH/H_2O/C_{35}H_{71}OH$ ) was also carried out [Fig. 3(b)]. The resulting value of  $D_{MD} \approx 0$  is in agreement with our experimental reflectivity data for 1-triacontanol ( $C_{30}H_{61}OH$ ),  $D_{exp} \approx 0$ .

One of the fundamental questions is how the water molecules adapt to the density depression. To elucidate the structural orientation, we have monitored the water dipole moments as a function of the distance from the interface [27]. Figure 3(iii) shows this in terms of  $P(z) = \langle \cos(\theta) \rangle$ , the average projection of the normalized water dipole moment on the surface normal, plotted versus  $z$ , the coordinate normal to the interface. One sees that the first two monolayers of water molecules in direct contact with the paraffin interface exhibit some degree of preferred orientation: Nearest to the alkanes the water dipole moments (and thus the hydrogens) tend to point more towards the alkanes than away from them. In the next layer the effect is smaller and opposite. Farther from the interface the water orientation is isotropic. For the simulation of the alcohol water system, the orientations are opposite in the first two layers and the ordered layers persists over more than two monolayers.

The same MD data can be compiled into the probability of observing a given dipole orientation [ $\cos(\theta)$ ] at position  $z$  which in turn can be translated into an orientational entropy in excess of random water amounting to  $0.027 \text{ mJ}/(\text{m}^2 \text{ K})$  [27]. This value is equivalent to a surface free energy at 300 K of  $8 \text{ mJ}/\text{m}^2$  which in turn is only 8% of the entropic contribution to the change in free energy if a monolayer of ice were melted (i.e.,  $100 \text{ mJ}/\text{m}^2$ ) or 16% of the free energy of a hydrophobic surface in contact with water ( $55 \text{ mJ}/\text{m}^2$ , cf. below) [10]. The contribution of this orientational effect to the total interfacial free energy is hence expected to be of minor importance despite the distinct peaks in the  $P(z)$  versus  $z$  plot (Fig. 3).

As an estimate of the possible order of magnitude of the change in surface free energy caused by a density reduction to  $D_{exp} = 1 \text{ \AA}$  we calculate the change in free energy when an ideal 2-dimensional hydrophobic alkane surface ( $\beta = 118^\circ$ , [22]) is pushed vertically into water thereby creating new regions with diluted decompressed water. Assuming that decompression is the only source of free energy change, expected to amount to

$\gamma_{\text{paraffin,water}} - \gamma_{\text{paraffin,air}}$  because a paraffin-water interface is created at the expense of a paraffin-air interface, we use the isothermal compressibility of water ( $\kappa = 4.5 \times 10^{-10} \text{ m}^2/\text{N}$ ) and obtain  $11 \text{ mJ/m}^2$  for the decompression of a  $10 \text{ \AA}$  thick interfacial region to 90% of the bulk water density, and  $33 \text{ mJ/m}^2$  for decompression of a  $3 \text{ \AA}$  layer to 66% of the density of bulk water (in both cases  $D = 1 \text{ \AA}$  cf. [28]). These crude estimates compare surprisingly well with the change in interfacial free energy obtained from Young's equation using appropriate values of  $\beta_{\text{paraffin}} = 118^\circ$  and  $\gamma_{\text{water,air}} = 72 \text{ mJ/m}^2$  ( $\gamma_{\text{paraffin,water}} - \gamma_{\text{paraffin,air}} = 34 \text{ mJ/m}^2$ ) [10].

In summary we have shown experimentally that an intrinsic dewetting of large hydrophobic surfaces in water occurs ( $D_{\text{exp}} = 1 \text{ \AA}$ ). The effect is significantly smaller than predicted by those theoretical models ( $D_{\text{theory 1}} = 10 \text{ \AA}$ ) [1,3,5] which exclude attractive interactions between water and the hydrophobic wall while it is larger than recent estimates which include attractive interactions ( $D_{\text{theory 2}} = 1/2 \text{ \AA}$ ) [4,5]. Estimates of the contribution to the free energy of creating the diluted interfacial region show that dilution may contribute very significantly to the interfacial free energy of hydrophobic surfaces in water. Our own MD simulations suggest an extensive dilution at the interface actually creating a thin ( $1 \text{ \AA}$ ) "vacuum" layer. The observed temperature dependence and the results of our MD simulations ( $D_{\text{MD}} = 1 \text{ \AA}$ ) indicate that orientational (entropic) effects play a minor role.

The authors wish to thank Jens Als-Nielsen, Ole G. Mouritsen, Sven Bjørnholm, Flemming Yssing Hansen, Alenka Luzar, and Håkan Wennerström for fruitful discussions. The project received financial support from the Danish National Research Council including the DanSync program and from the European Community (IHP-Contract No. HPRI-CT-1999-00040). In addition we are grateful for beam time at the HASYLAB Synchrotron Laboratory.

\*Present address: Department of Chemistry, University of Aarhus, DK-8000 Århus C, Denmark.

†Present address: Quantum Protein Centre, Department of Physics, Technical University of Denmark, DK-2800 Lyngby, Denmark.

‡Corresponding author.

Email address: tb@nano.ku.dk

- [1] F. H. Stillinger, *J. Solution Chem.* **2**, 141 (1973).
- [2] K. Lum and A. Luzar, *Phys. Rev. E* **56**, 6283 (1997).
- [3] K. Lum, D. Chandler, and J. D. Weeks, *J. Phys. Chem. B* **103**, 4570 (1999).
- [4] A. Luzar and K. Leung, *J. Chem. Phys.* **113**, 5836 (2000).
- [5] A. Wallqvist, E. Gallicchio, and R. M. Levy, *J. Phys. Chem. B* **105**, 6745 (2001).
- [6] H. S. Ashbaugh and M. E. Paulaitis, *J. Am. Chem. Soc.* **123**, 10 721 (2001).
- [7] D. Bratko, R. A. Curtis, H. W. Blanch, and J. M.

Prausnitz, *J. Chem. Phys.* **115**, 3873 (2001).

- [8] D. Leckband and J. Israelachvili, *Q. Rev. Biophys.* **34**, 105 (2001).
- [9] O. C. Tanford, *The Hydrophobic Effect: Formation of Micelles and Biological Membranes* (Wiley & Sons, New York, 1980).
- [10] J. Israelachvili, *Intermolecular & Surface Forces* (Academic Press, London, 1992).
- [11] V. V. Yaminsky and E. A. Vogler, *Curr. Opin. Colloid Interface Sci.* **6**, 342 (2001).
- [12] A. Terfort, N. Bowden, and G. M. Whitesides, *Nature (London)* **386**, 162 (1997).
- [13] H. S. Frank and M. W. Evans, *J. Chem. Phys.* **13**, 507 (1945).
- [14] A. Luzar, *Chem. Phys. Lett.* **96**, 485 (1983).
- [15] Q. Du, E. Freysz, and Y. R. Shen, *Science* **264**, 826 (1994).
- [16] A. Wallqvist and B. J. Berne, *J. Phys. Chem.* **99**, 2885 (1995).
- [17] J. Israelachvili, *Surf. Sci. Rep.* **14**, 109 (1992).
- [18] S. P. Weinbach *et al.*, *Adv. Mater.* **7**, 857 (1995).
- [19] J. Als-Nielsen *et al.*, *Phys. Rep.* **246**, 251 (1994).
- [20] For  $\rho(z)$  (inverted from the reflectivity data) the errors were estimated by taking into account the counting errors on the raw data, formally propagated in the inversion procedure [21], as well as the variation between  $\rho(z)$  curves that result from different choices of the stabilization parameters of the inversion procedure [21] but which all correspond to good fits to the measured reflectivity data.
- [21] J. Skov-Pedersen and I. W. Hamley, *J. Appl. Crystallogr.* **27**, 36 (1994).
- [22] C. D. Bain and G. M. Whitesides, *Angew. Chem., Int. Ed. Engl.* **28**, 506 (1989).
- [23] J. Forsman, B. Jönsson, C. E. Woodwarf, and H. Wennerström, *J. Phys. Chem. B* **101**, 4253 (1997).
- [24] L. Kale *et al.*, *J. Comput. Phys.* **151**, 283 (1999).
- [25] M. Schlenkrich, J. Brinckmann, Jr., A. D. MacKerell, and M. Karplus, in *Biological Membranes*, edited by K. M. Merz and B. Roux, A Molecular Perspective from Computation and Experiment (Birkhauser, Boston, 1996), p. 31.
- [26] T. Darden, D. York, and L. Pedersen, *J. Chem. Phys.* **98**, 10 089 (1993).
- [27] M. Ø. Jensen, O. G. Mouritsen, and G. H. Peters (to be published).
- [28] We estimate the energy needed to *compress water* by 10% at constant temperature using the isothermal compressibility of water  $\kappa = (1/V)(dV/dP) \approx (1/V)(\Delta V/\Delta P)$ . If  $\Delta V/V = 0.1$  then  $\Delta P = 0.1/\kappa = 2.2 \times 10^8 \text{ N/m}^2$  using  $\kappa = 4.5 \times 10^{-10} \text{ m}^2/\text{N}$ . The corresponding work  $W$  is approximated by  $W = \int PdV \approx (1/2)\Delta P\Delta V$ . For the interfacial region we set  $V = Ad$  where  $d$  is the thickness and  $A$  the area of the interface. This gives  $W = (1/2)\Delta PAd$  and the work per unit area  $W/A = (1/2)\Delta Pd = (1/2)(2 \times 10^8 \text{ N/m}^2)(1 \times 10^{-10} \text{ m}) = 11 \text{ mJ/m}^2$ . Using the same procedure for  $\Delta V/V = 0.3$  we get  $W/A = 33 \text{ mJ/m}^2$ . We assume that the energy required for a *decompression* of water is of the same order of magnitude due to the symmetry of the interaction potential between the molecules in the vicinity of the global minimum.